RED BLOOD CELL ORIENTATION IN ORBIT $C = 0$

M. BITBOL

Laboratoire de Biorhéologie et d'Hydrodynamique Physico-chimique (Laboratoire Associé au Centre National de la Recherche Scientifique, LA 343), Université Paris VII, 75251, Paris Cedex 05, France

ABSTRACT Two modes of behavior of single human red cells in a shear field have been described. It is known that in low viscosity media and at shear rates $<20\ s^{-1}$, the cells rotate with a periodically varying angular velocity, in accord with the theory of Jeffery (1922) for oblate spheroids. In media of viscosity $>\sim 5$ mPa s and sufficiently high shear rates, the cells align themselves at a constant angle to the direction of flow with the membrane undergoing tank-tread motion. Also, in low viscosity media, as the shear rate is increased, more and more cells lie in the plane of shear, undergoing spin with their axes of symmetry aligned with the vorticity axis of the shear field in an orbit "$C = 0$" (Goldsmith and Marlow, 1972). We have explored this latter phenomenon using two experimental methods. First, the erythrocytes were observed in the rheoscope and their diameters measured. Forward light scattering patterns were correlated with the red cell orientation mode. Light flux variations after flow onset or stop were measured, and the characteristic times of erythrocyte orientation and disorientation were assessed. The characteristic time of erythrocyte orientation in Orbit $C = 0$ is proportional to the inverse of the shear rate. The corresponding coefficient of proportionality depends on the suspending medium viscosity η_o. The disorientation time τ_D, after flow has been stopped, is such that the ratio τ_D/η_o is independent of the initial applied shear stress. However, τ_D is much shorter than one would expect if pure Brownian motion were involved. The proportion of erythrocytes in orbit $C = 0$ was also measured. It was found that this proportion is a function of both the shear rate and η_o. At low values of η_o, the proportion increases with increasing shear rate and then reaches a plateau. For higher values of η_o (5 to 10 mPa s), the proportion of RBC in orbit $C = 0$ is a decreasing function of the shear stress. A critical transition between orbit $C = 0$ and parallel alignment was observed at high values of η_o, when the shear stress is on the order of 1 N/m^2. Finally, the effect of altering membrane viscoelastic properties (by heat or diamide treatment) was tested. The proportion of oriented cells is a steep decreasing function of red cell rigidity.

INTRODUCTION

It has long since become well known that red blood cells in a shear field can orient themselves almost parallel to the flow direction (1). It is the tank-treading motion (2, 3) of the membrane around the cell content which enables the erythrocyte to take on a stable orientation. The transition threshold of the RBC from a flipping motion to a definite orientation has been demonstrated to depend both on the viscosity ratio[1] η_i/η_o, and the erythrocyte elongation (4, 5). (η_i is the internal viscosity and η_o the suspending medium viscosity.) The influence of high concentrations on these phenomena has also been studied (6–8). Yet, the flipping and tank-treading motions of red cells are not the only possible ones. While studying the differences in behavior between normal and hardened red blood cells in a flow, Goldsmith and Marlow (9) observed that when the shear rate in plasma-Ringers was increased, the cells spent more time aligned with the flow during each orbit than predicted by theory for a rigid spheroid. At the same time, an increasing number of cells drifted into an orbit "$C = 0$" in which the axis of symmetry is aligned with vorticity axis, and the cells exhibit spin without angular rotation. Moreover, it was shown by the authors that the fraction of normal erythrocytes in this orbit at a given shear rate was appreciably greater than that of hardened cells. Until now, however, very little attention has been paid to this phenomenon, in spite of its obvious relationship with red cell deformability. It is the purpose of the present paper to study the characteristic behavior of red blood cells in orbit $C = 0$. We shall first afford, in the following section, a short historical sketch of the concept of orbital motion when applied to rigid ellipsoids or disks. The next section is devoted to the description of the experimental methods, and finally the results of both direct rheoscope observation and light scattering measurements will be given.

ORBITAL MOTION OF A RIGID ELLIPSOID OR DISK

The fundamental theoretical work on the motion of a rigid ellipsoid in steady flow was performed by Jeffery in 1922 (10). By computing the

Dr. Bitbol's present address is Institut de Biologie Physico-chimique, 13, Rue Pierre et Marie Curie, 75005 Paris, France.

[1] c.g.s. équivalents to the M.K.S.A. Units used in the text: volume viscosity, 1 mPa s = 10^2 Poise = 1 Centipoise; shear stress, 1 N/m^2 = 10 dynes /cm^2; surface viscosity, 1 mPa s × m = 1 Poise × cm = 1 dyne × cm/s.

hydrodynamic torque exerted on the ellipsoid, and setting it equal to 0, the author found two formulas for the time dependence of the angular variables θ and ϕ (see Fig. 1). For an ellipsoid of revolution, the half axes of which are a and b (a being the half length of the axis of symmetry, and b the half diametrical axis), we have

$$\tan\phi = r_e \tan\left(\frac{\dot{\gamma}t}{r_e + r_e^{-1}}\right), \tag{1a}$$

where $r_e = a/b$ is the axis ratio, and $\dot{\gamma}$ the shear rate. The function $\theta(t)$ is then given by

$$\tan\theta = \frac{Cr_e}{(r_e^2\cos^2\phi + \sin^2\phi)^{1/2}}, \tag{1b}$$

where C is referred to as the orbit constant. It is positive, and depends only on the initial position of release of the ellipsoid (notice that in Jeffery's original work the constant $k = b/C$ was used instead of C. The parameter C was first introduced by Trevelyan and Mason (11). Moreover, the ellipsoid undergoes spin around its axis of revolution, given by:

$$|\vec{\omega}| = \frac{\dot{\gamma}}{2}\cos\theta. \tag{2}$$

According to Eq. 1A, a prolate rigid ellipsoid spends more time near to an angle $\phi = (2n + 1)(\Pi/2)$ than near to $\phi = n\Pi$, while an oblate ellipsoid spends more time in the vicinity of $\phi = n\Pi$ (n being an integer). In both cases, therefore, the ellipsoid spends more time with its major axis close to the direction of the streamlines than across the streamlines. Furthermore, it follows from Eq. 1B that while ϕ increases from 0 to Π, and from Π to 2Π, θ varies between angles θ_1 and θ_2:

$$\tan\theta_1 = Cr_e \quad \left(\text{for } \phi = (2n + 1)\frac{\Pi}{2}\right)$$

$$\tan\theta_2 = C \qquad (\text{for } \phi = n\Pi). \tag{3}$$

Finally, one must notice that the orbit constant C may take on values between the limits 0 ($\theta = 0$ at all ϕ) corresponding to steady spin of the axis of symmetry about the vorticity axis at a rate $\omega = \dot{\gamma}/2$, and ∞($\theta = \Pi/2$ at all ϕ) corresponding to variable $d\phi/dt$ without axial spin. The validity of Eqs. 1A, 1B, and 2, initially demonstrated for ellipsoids, was eventually extended to other bodies with more general shape. Indeed, Bretherton (12) showed that the motion of any particle having a symmetry axis can be described in a similar way, provided an equivalent ellipsoid axis ratio, r_e, is defined for each particle. This equivalent ratio is greater than the particle axis ratio, r_p, for disks, and smaller for rods (13). Its value for human red blood cells was found to be: $r_e = 0.38 \pm 0.07$ (9). But this simple model of particle motion was soon challenged. According to it, all values of C between 0 and ∞ are equally possible, and there is no way to determine the relative probability of these orbit constants, nor to predict any orbital drift. Jeffery recognized that this indeterminacy was the result of the approximation of creeping flow used in his development. He pointed out at the end of his paper that "a more complete investigation would reveal the fact that the particles do tend to adopt special orientations with respect to the motion of the surrounding fluid. The suggestion is that the particles will tend to adopt that motion which, of all the motions possible under the approximated equations, corresponds to the least dissipation of energy." As it was already demonstrated in Jeffery's paper (10), the motion that gives minimum overall energy dissipation corresponds to $\theta = \Pi/2$ (i.e., $C = \infty$) for an oblate ellipsoid. This is also true for disks and hardened red blood cells (13). In 1956, Saffman (14) tried to demonstrate Jeffery's conjecture about the orbital drift. First, he showed that no orbital drift can take place in a creeping motion, described by the Stokes equation. This is due to the fact that Stokes equation being symmetric under time reversal, no preferential direction of drift can be defined (for a general form of this theorem, see Bretherton, 12). Then, by taking into account first order inertial terms, Saffman was led to the equation (originally written in terms of k, and not C):

$$-\frac{1}{C}\frac{dC}{dt} = \frac{a\dot{\gamma}^2(a - b)\rho}{\eta_0}\cdot f\left(\frac{C}{a}\right), \tag{4}$$

ρ being the suspending fluid density, η_0 its viscosity, and f a positive function of (C/a). Notice that for an oblate ellipsoid, i.e. when $a < b$, $(dC/dt) > 0$ and thus $C \to \infty$. The latter result is in good agreement with Jeffery's prediction. However, in a very accurate experimental investigation bearing on disks and rods flowing either in a Couette or in a Poiseuille velocity profile, Karnis et al. (15) observed that disks drift towards orbit $C = 0$, i.e. $\theta = 0$ at all ϕ. This is the orbit of maximum dissipated energy. Although their experimental outcome directly contradicted Saffman's calculations, the authors did not recognize this major discrepancy, due to their misinterpretation of Eq. 4. Nevertheless, they did notice another discrepancy between their experimental results and Eq. 4: the rate at which disks became oriented in the flow was not proportional to $\dot{\gamma}^2$. Clearly, a satisfactory theory for the problem of rigid disk orbital drift has not yet been found. In the present investigation, the fact that red blood cells are flexible is an additional unwelcome intricacy. From an experimental standpoint however, the normal erythrocyte orbital drift is simple to describe. We will proceed in the following to give such a description.

MATERIAL AND METHODS

Preparation of Blood

Blood was drawn by venipuncture on E.D.T.A. from young healthy subjects. It was first centrifuged at 1,000 g. The plasma and the buffy coat were removed, and then the pellet was washed twice in phosphate buffered saline (PBS) pH 7.4 containing 1 g/l glucose. After that, a given volume of washed pellet was added to a suspending medium made of PBS + Dextran T 40 (Pharmacia Fine Chemicals, Piscataway, NJ). The Dextran concentration was adjusted to obtain a viscosity ranging between 1 and 10 mPa s. The hematocrit we used throughout this work (except for a particular experiment aiming at testing the effect of RBC volume concentration on disorientation time) was 0.5%.

Three types of treatment were used to modify the RBC viscoleastic properties. With the first one, the red cells were completely hardened by glutaraldehyde. The procedure consisted in preparing first a 20% suspension of washed erythrocytes in PBS. Then, an equal volume of PBS + glutaraldehyde 5% solution was added slowly (in 1 h) to the continuously stirred suspension (16). This leads finally to a 10% suspension in a 2.5% glutaraldehyde solution. Cell shape was checked under the microscope and it was noticed that most erythrocytes were normal discocytes. Two hours later, the remaining suspension was centrifuged and a sample of the pellet was resuspended in the viscous medium. The purpose of the second procedure was to create a network of disulfide bridges in membrane proteins by diamide treatment. The method used was exactly the one described by Fischer et al. (17). The concentration of diamide was varied between 0.05 mM and 0.2 mM. In the third procedure heat treatment was used to alter the membrane deformability (18). Erythrocyte suspensions at 40% hematocrit in 5 ml tubes were maintained for 2 to 12 min, in a heated water bath at 48.7 ± 0.2°C, and stirred gently.

Rheoscope Observations, and Optical Measurements

(a) The observations were performed on a cone-plate rheoscope. The cone angle was 1.5°, and the shear rate ranged between 1 and 200 s^{-1}. Many photographs were taken with a 35 mm camera, for several values of suspending medium viscosity and shear rate. The diameters of red cells in orbit $C = 0$ were measured according to Ponder's rule (see 19) i.e., by locating the external boundary of the erythrocyte shadow in an edge-on position. About 10 to 20 RBC diameters were measured for each pair of values $(\eta_0, \dot{\gamma})$.

(*b*) Pictures of simple light forward scattering patterns through flowing erythrocyte suspensions were taken. In this experiment a laser beam (He-Ne, 6328 Å; Spectra-Physics, Inc., Mountain View, CA) crossed perpendicularly a plane Poiseuille flow. Such a flow pattern was obtained by making the suspensions go through a plexiglas channel whose cross-section is rectangular, with one dimension much larger than the other (15 × 0.3 mm). The average shear-rate was calculated by the following formula:

$$\langle \dot{\gamma} \rangle = \frac{3Q}{e^2 l}, \tag{5}$$

where Q is the flow rate, e the length of the smaller dimension, and l the length of the larger one.

(*c*) The forward scattered light flux was then measured by focusing part of it onto a photodiode. The axis joining the center of the converging lens with the photodiode is set within the plane containing both the laser beam and the flow velocity vector which originates at the light spot (Fig. 2). The angle θ' between this axis and the laser beam was varied between 0 and 20° with a collection aperture ±1.1°, due to the finite lens diameter. As we sought to measure the orientation and disorientation times, we focused our attention on light flux variation after the flow onset or after its stop. Finally, we also performed the same measurements of forward scattered light flux across RBC suspensions in a Couette flow, by means of an ektacytometer (20).

RESULTS

Rheoscope Observations

To understand the meaning of these observations, notice that they were made in the plane xz defined in Fig. 1, whereas Goldsmith and Marlow observed the cells in the xy plane (9). Four types of red cell flow behavior were seen.

At rest, the sedimentation process was fast enough such as to deposit the erythrocytes onto the bottom plate of the rheoscope in a few seconds. In Fig. 3 *a*, the red cells are seen face-on after settling. If the vertical dimension of the container had been large enough to allow the red cells to remain suspended during several minutes, as is the case in our rectangular channel and in Couette device, randomly oriented erythrocytes would have been observed (see below).

At very low shear stresses ($\eta_0\dot{\gamma} < 0.02$ N/m^2), the red cells rotate in the flow.

At intermediate shear stresses ranging approximately between 0.02 N/m^2 and 1 N/m^2 the RBC symmetry axis drifts towards the vorticity axis, and then the erythrocytes are seen edge on (Fig. 3 *b*), spinning in the orbit $C = 0$.

For higher values of the shear stress ($\eta_0\dot{\gamma} \geq 1$ N/m^2), the orbit $C = 0$ becomes unstable, and the red cells align almost parallel to the rheoscope plate, with varying degrees of elongation (Fig. 3 *c*). It is in this position that the tank-treading motion occurs.

The result of RBC diameter measurements in orbit $C = 0$ is plotted in Fig. 4 as a function of shear rate, for two suspending medium viscosities: 2 mPa s and 7.3 mPa s. The standard deviation for each point is of order 10% of the mean diameter value. This is consistent with previous measurements of red cell diameter at rest (9). In spite of the fact that the standard deviation is of the same magnitude as the maximum erythrocyte elongation, it was possible to demonstrate with a Student's t test that this elongation is statistically significant. When $\eta_0 = 7.3$ mPa s, the diameter of red blood cells in orbit $C = 0$ is significantly higher than the diameter at rest ($P < 0.01$) for a shear rate value of 21 s^{-1}. When $\eta_0 = 2$ mPa s, the same result (but with $P < 0.05$) is reached at 45 s^{-1}. An interpretation of these results will be given in the discussion.

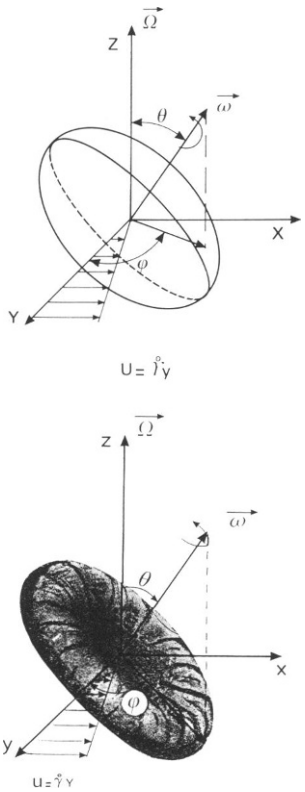

FIGURE 1 Polar coordinates for an ellipsoid (*a*) and a red blood cell (*b*) in shear flow.

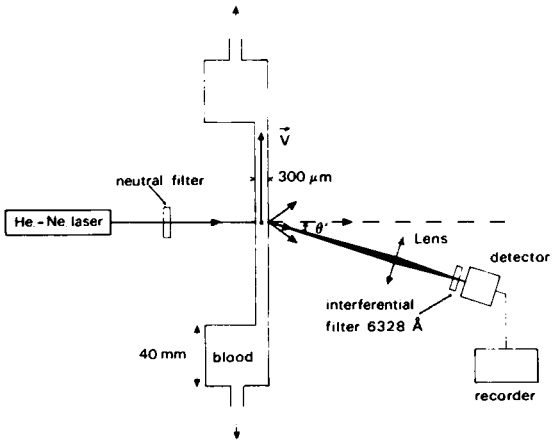

FIGURE 2 Forward scattered light flux measurements across a plexiglas channel. The channel cross section has the following dimensions: 15 × 0.3 mm.

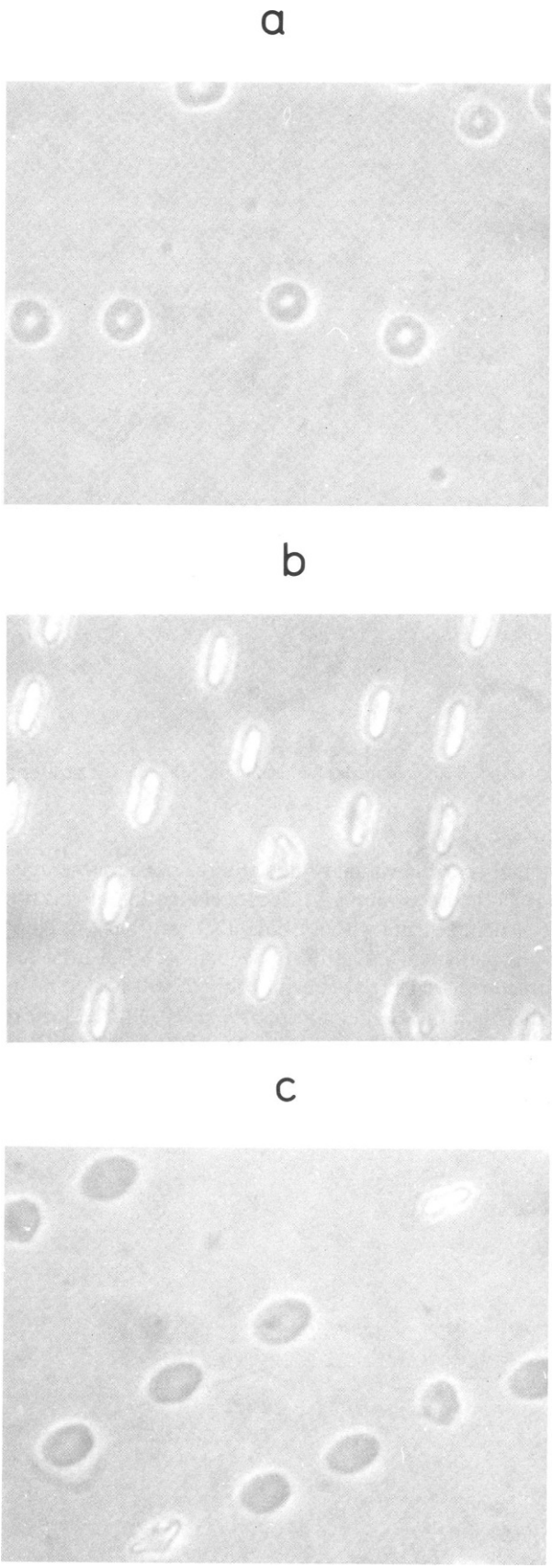

FIGURE 3 Red blood cells in a rheoscope, at hematocrit 0.5%. (*a*) at rest; (*b*) η_o = 4 mPa s, $\eta_o\dot{\gamma}$ = 0.2 N/m^2; (*c*) η_o = 10 mPa s, $\eta_o\dot{\gamma}$ = 2N/m^2. The overall direction indicated by the edge-on cells (*b*) and the tank-treading cells (*c*) is identical to the flow direction. The fact that the angle between this direction and the sides of the photograph can vary is due to practical reasons.

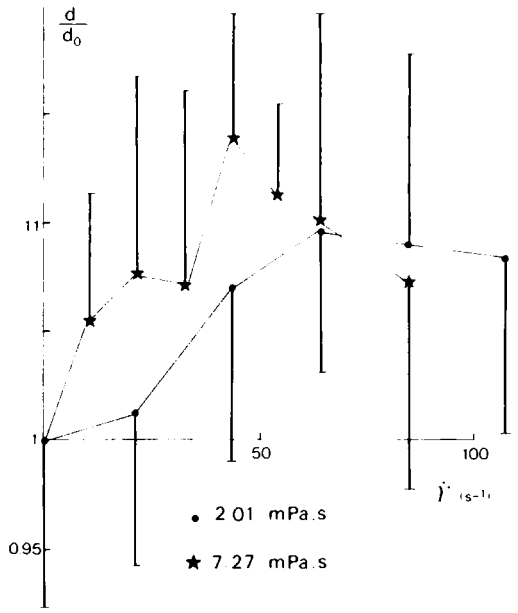

FIGURE 4 RBC diameter in orbit $C = 0$ (related to the diameter at rest) vs. shear rate. Each point is the average of 10 to 20 diameter measurements.

Forward Light Scattering Pattern

There exists a direct and simple correspondence between the various states of RBC orientation as they were described above, and the light scattering patterns. At zero shear rate, the red cells are randomly oriented and the scattering pattern is merely circular (Fig. 5 *a*). When a considerable proportion of erythrocyte are spinning in orbit $C = 0$, the scattering pattern elongates perpendicular to the red cell edge. Fig. 5 *b* shows a pattern obtained for η_o = 17 mPa s and $\eta_o \langle\dot{\gamma}\rangle = 0.17$ N/m^2. Notice, however, that part of this scattered light pattern exhibits a circular symmetry, due to the fact that a certain proportion of erythrocytes still tumble in the flow. When the shear stress is moderately increased (Fig. 5 *c*, η_o = 17 mPa s and $\eta_o\langle\dot{\gamma}\rangle = 0.6$ N/m^2), the scattering pattern again becomes circular as the red cells become oriented almost parallel to the plane of equal velocity vectors, and are very slightly deformed. Finally, at very high shear stress (Fig. 5 *d*, η_o = 17 mPa s, $\eta_o\langle\dot{\gamma}\rangle = 42$ N/m^2) the light scattering pattern elongates again because of the corresponding red cell elongation (20). The detailed study of the scattering patterns could potentially provide a considerable amount of information about RBC orientation phenomena. However, a theoretical understanding of simple light scattering by nonspherical intermediate size particles would be required. Attempts to develop such a theory have failed to produce usable formulas (21). In the following, we will limit our study to several light flux measurements at specific scattering angles.

Light Flux Measurements

The shape of light flux variation curves after flow onset depends very strongly on the measurement angle θ' with

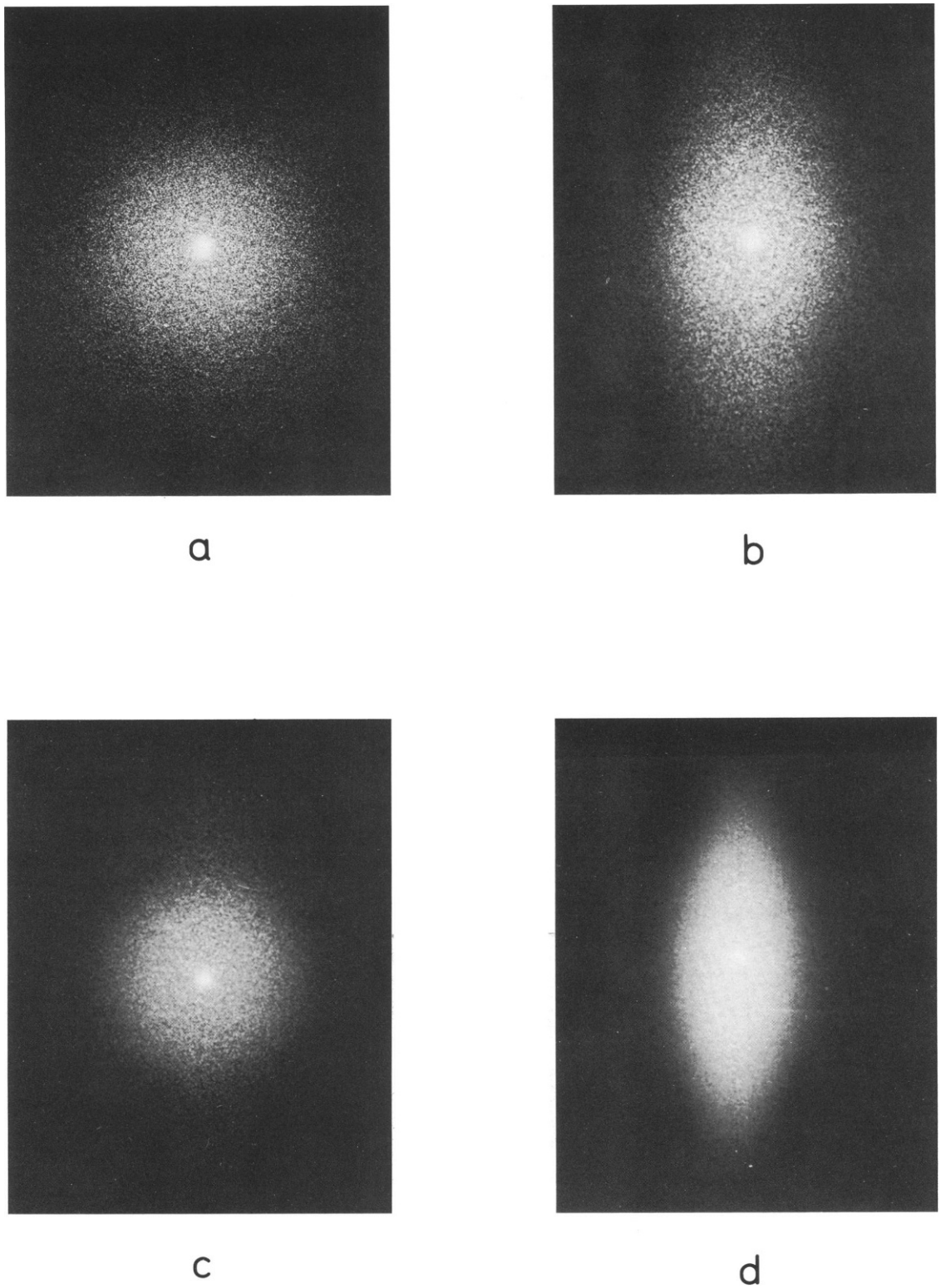

FIGURE 5 Light forward scattering patterns across a plane Poiseuille flow. (*a*) at rest; (*b*) $\eta_o = 17$ mPa s, $\eta_o \langle \dot{\gamma} \rangle = 0.17$ N/m^2; (*c*) $\eta_o = 17$ mPa s, $\eta_o \langle \dot{\gamma} \rangle = 0.6$ N/m^2; (*d*) $\eta_o = 17$ mPa s, $\eta_o \langle \dot{\gamma} \rangle = 42$ N/m^2.

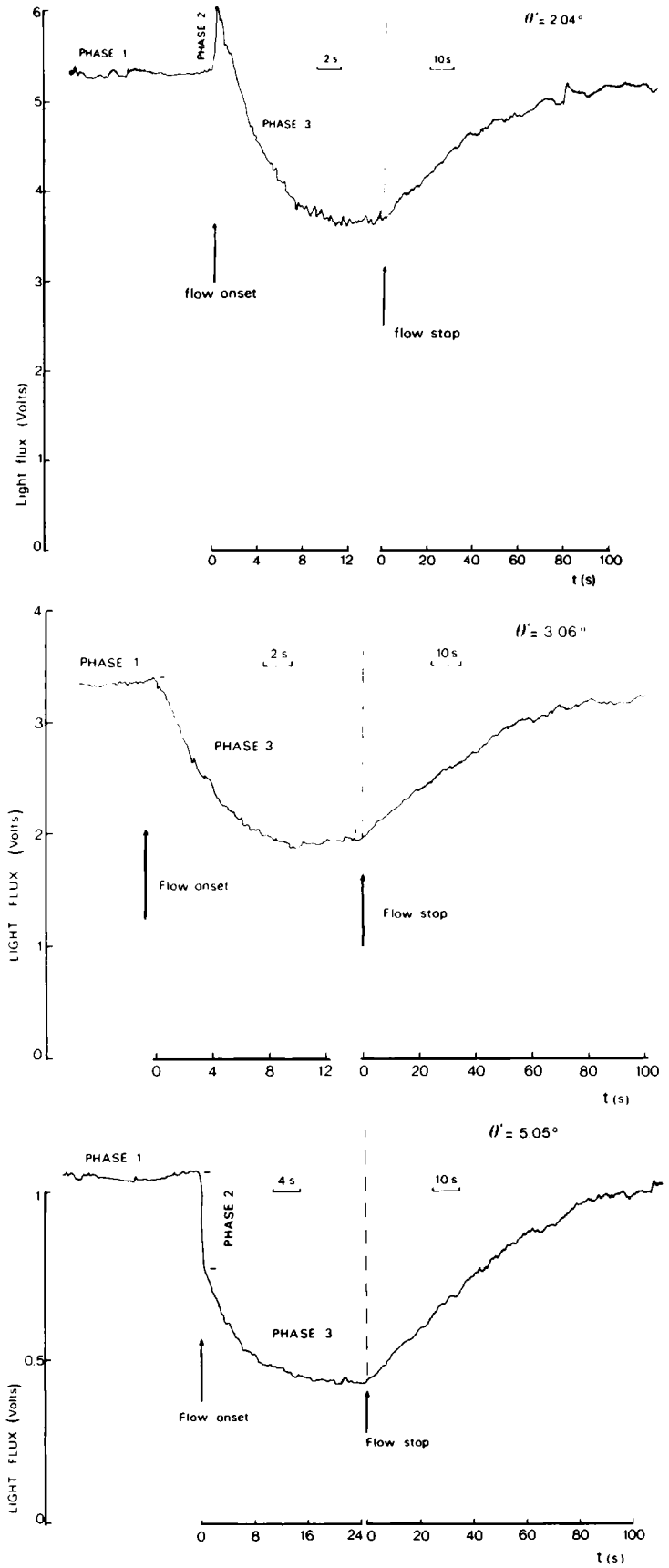

FIGURE 6 Light flux variation curves after flow onset and flow stop. η_o = 2 mPa s, $\eta_o \langle \dot{\gamma} \rangle$ = 0.076 N/m^2. (*a*) θ' = 2.04°; (*b*) θ' = 3.06°; (*c*) θ' = 5.05°. At θ' = 2.04°, "phase 2" is a light flux increase, while at θ' = 5.05 it is a decrease. At θ' = 3.06°, this "phase 2" disappears. This disappearance corresponds to the intersection of the "phase 1" and "phase 2" scattering curves as shown in Fig. 7.

respect to the laser beam direction. In Figs. 6 *a*, *b*, and *c*, we have plotted three such curves obtained at different angles (θ') under fixed rheological conditions (η_0 = 2 mPa s and $\eta_0\langle\dot{\gamma}\rangle$ = 0.076 N/m^2). In Fig. 6 *a* (θ' = 2.04°), there is a sudden increase in the light flux after the flow onset (phase 2 on the figure). This phenomenon has been documented previously (see e.g., [22]). It corresponds to the initial rotation of the red cells as they become aligned parallel to the plane of equal velocity vectors in a time of order $\dot{\gamma}^{-1}$ (see Eq. 1A). During the subsequent period (phase 3) the light flux decreases quite slowly towards an asymptotic value. This decrease is related to an elongation of the scattering pattern similar to that of Fig. 5 *b*. It, therefore, reflects the progressive drift of red cells towards orbit C = 0. Finally, after the flow has been stopped, the light flux increases again very slowly and approaches a baseline value corresponding to randomly oriented cells. In Figs. 6 *b* and *c*, (θ' = 3.06° and θ' = 5.05°, respectively) a different behavior is observed in phase 2. At θ' = 3.06° there is almost no change in the light flux immediately after flow onset, and at θ' = 5.05°, there is a rapid decrease in the flux. The angular dependence of scattered light flux is shown in Fig. 7 for the same rheological parameters as in Fig. 6. Each curve was in this case obtained by measuring the value of light flux at the end of the three phases of Fig. 6. The "phase 1" curve gives the angular dependence of light flux scattered by a randomly oriented RBC suspension. The "phase 2" curve corresponds to an increase in the number of red cells aligned with the flow (i.e., $\phi \simeq 0$ and $\theta = \Pi/2$, ϕ and θ defined in Fig. 1). When part of the erythrocytes are aligned with the flow, their symmetry axis is parallel to the light beam, and their light-scattering cross-section is minimum (22). Therefore, the "phase 2" scattering pattern is narrower and brighter in the center than the "phase 1" pattern that corresponds to randomly oriented RBC. The intersection between "phase 1" and

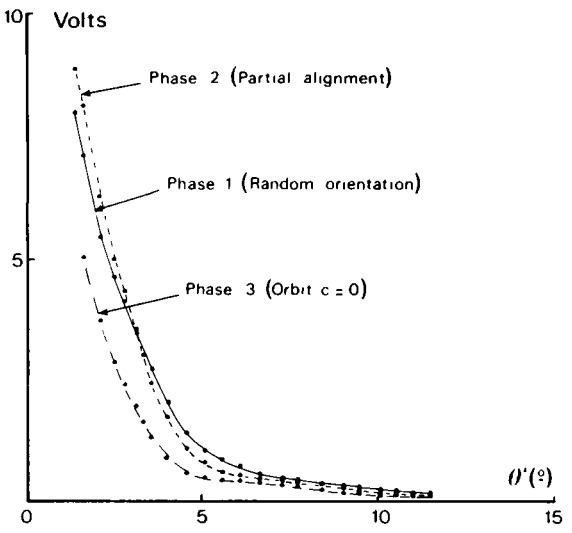

FIGURE 7 Scattered light flux vs. angle θ', at the end of the three phases defined in Fig. 6.

"phase 2" curves takes place at $\sim\theta'$ = 3°, as expected from Fig. 6 *b*. As for the "phase 3" curve, it is clearly lower than the others: this is due to a light flux decrease in the measurement plane, when the scattering pattern becomes elongated. It is possible to estimate the proportion of erythrocytes in orbit C = 0 from the difference in light flux between phase 1 and the two other phases of Fig. 6. Let us denote the light flux difference between the end of phase 2 and the end of phase 3 by Δr_{C-0}, while the total light flux difference between phase 1 and the end of phase 3 is denoted by Δr_T. We can then seek empirically the particular value of angle θ' such that $\Delta r_{C-0}/\Delta r_T$ becomes quantitatively close to the ratio n_{C-0}/n_T, where n_{C-0} is the number of red cells in orbit C = 0 and n_T is the total number of oriented erythrocytes either parallel to the flow or in orbit C = 0. The latter data are available in Goldsmith and Marlow's original paper (9). They were obtained by direct observations of red cells suspended in Ringer's solutions, and flowing in a Poiseuille profile. The authors then gave the proportion P_{C-0} of erythrocytes in orbit C = 0, and the proportion P_0 of the erythrocytes whose angle ϕ ranges between +20° and −20° among those that are not in orbit C = 0. $P_{C-0}/[P_0(1 - P_{C-0}) + P_{C-0}]$ is thus equal to n_{C-0}/n_T. In Fig. 8, we have plotted both our light flux ratio $\Delta r_{C-0}/\Delta r_T$ at θ' = 5.05°, for red cells in PBS, and Goldsmith and Marlow's direct observations in the form n_{C-0}/n_T. One can see that there exists good agreement between the two sets of data. Hence, we shall consider the values $\Delta r_{C-0}/\Delta r_T$ for θ' = 5.05° to be a good estimate of the ratio n_{C-0}/n_T. This working hypothesis has also been confirmed qualitatively for several suspending media by comparing the proportions of oriented cells under the rheoscope, and $\Delta r_{C-0}/\Delta r_T$.

Orientation Time

The relaxation half-time (τ_0) of light flux decrease during phase 3, (i.e., during the phase of RBC drift towards orbit C = 0) was measured either in plane Poiseuille flow or in Couette flow. In Fig. 9, τ_0^{-1} is plotted vs. $\dot{\gamma}$ in Couette flow for several suspending medium viscosities η_0. The first result to be drawn from these data is that τ_0^{-1} at each η_0 is a linear function of $\dot{\gamma}$. This means that the rate of drift into C = 0 orbit increases linearly with shear rate. The constants of proportionality were then determined by obtaining the coefficients of the least squares straight lines which fit the experimental points. It was found that the slope of these straight lines is of order 10^{-2}, i.e., that the time of red cell drift towards orbit C = 0 is approximately ten times longer than a period of rotation $T = 2\Pi(r_e + r_e^{-1})\dot{\gamma}^{-1}$ (see Eq. 1). The behavior of red cells in plane Poiseuille flow does not depart very much from what is observed in Couette flow. Fig. 10 shows τ_0^{-1} plotted vs. $\langle\dot{\gamma}\rangle$ for plane Poiseuille flow. Again, there is a linear relationship between these two quantities. However, the dependence of the coefficient of proportionality on the suspending medium viscosity is not the same in plane

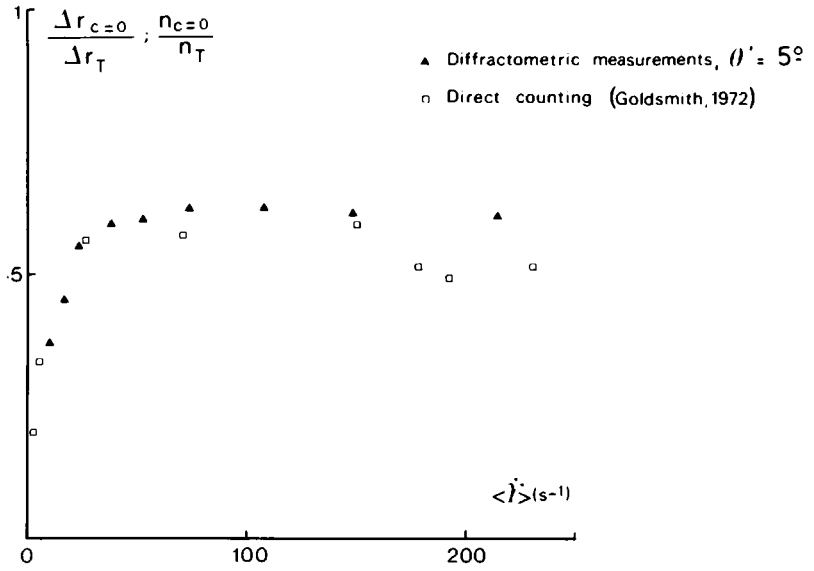

FIGURE 8 Comparison between the light flux variation ratio $\Delta r_{C=0}/\Delta r_T$ at $\theta' = 5.05°$ and direct counting of red cells in orbit $C = 0$.

Poiseuille flow as in Couette flow. In the latter case, the coefficient A is a monotonically increasing function of η_o, whereas in Poiseuille flow, it first increases, shows a maximum and then decreases (see Fig. 11). In interpreting these results, the reader should recognize that the larger A, the faster the drift at a given $\dot{\gamma}$.

Disorientation Time

If the return of very dilute red blood cell suspensions to random orientation after stop-flow is the result of Brownian motion, one would expect the ratio of the disorientation time to the suspending medium viscosity, τ_D/η_o, to be constant. As may be seen in Fig. 12, τ_D/η_o is indeed independent of the shear stress imposed just before stopping the flow. However, there are two discrepancies between the data shown in this figure and expectations for a Brownian motion driven disorientation. First, the ratio τ_D/η_o of hardened red cells is different from that of normal erythrocytes. Second, it will be shown in the discussion below that the two values of τ_D/η_o we obtained, i.e. 1.825 ×

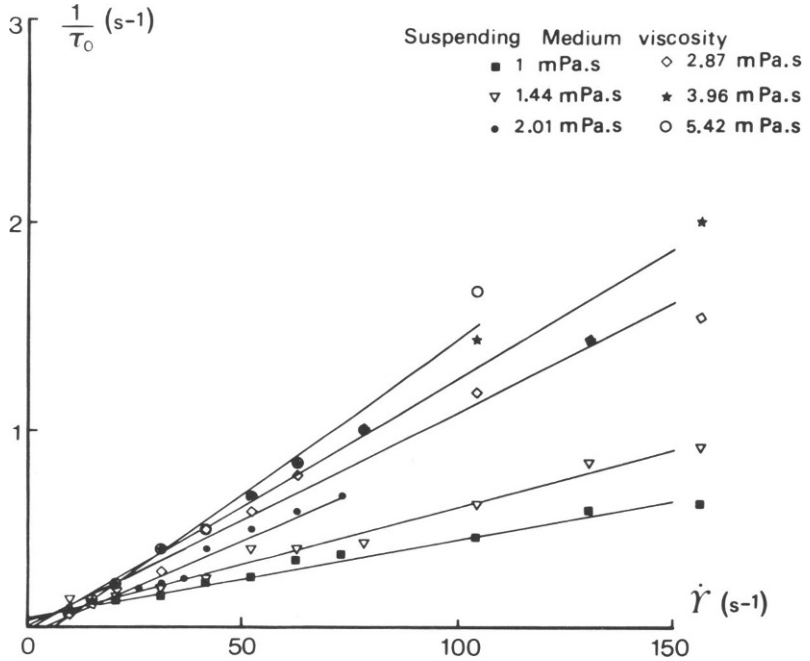

FIGURE 9 Inverse of RBC half time for orientation in orbit $C = 0$ vs. shear rate in Couette flow. The straight lines are fitted by the least-square method. We obtained similar straight lines for $\eta_o = 7.27$ mPa s and 9.68 mPa s, but they are not plotted in this figure in order to avoid confusion. However, their slope is represented in Fig. 11.

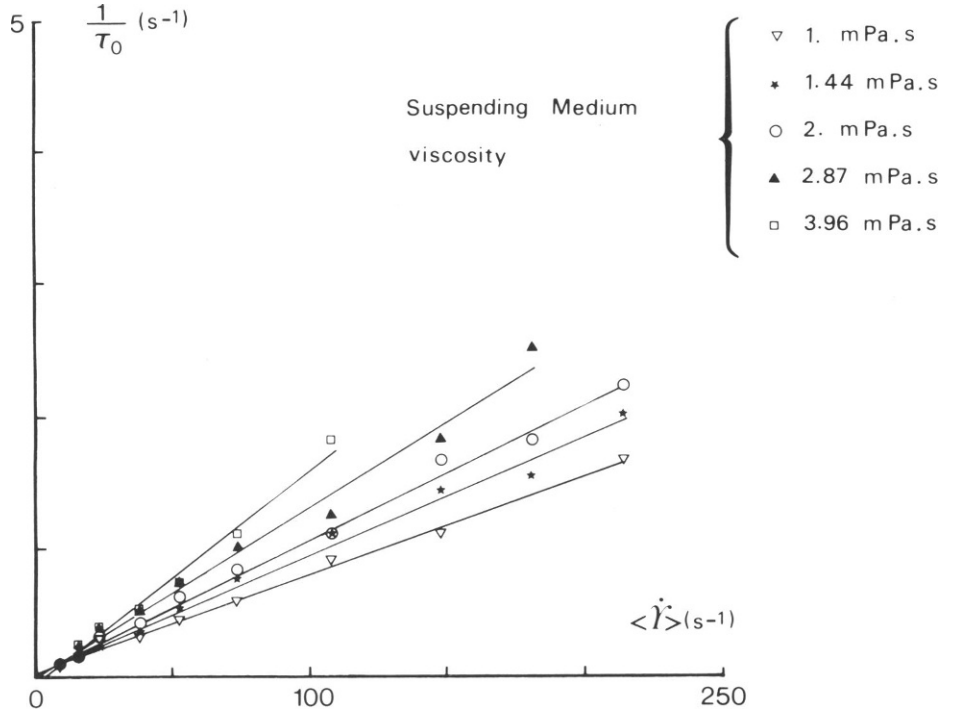

FIGURE 10 Inverse of RBC half time for orientation in orbit $C = 0$ vs. average shear rate in plane Poiseuille flow. Similar straight lines were obtained for $\eta_o = 7.27$ mPa s and 9.68 mPa s but they are not plotted in this figure. Their slope is represented in Fig. 11.

10^4 m^2/N and 1.17×10^4 m^2/N, are an order of magnitude too low to be accounted for by Brownian motion. Therefore, an alternate explanation for the RBC disorientation process must be found. One possibility is that the return to random orientation is due to RBC-RBC hydrodynamic interactions during sedimentation. A consequence of this assumption is that τ_D should decrease with increasing RBC concentration. Such a dependence is observed. Fig. 13 shows disorientation time measurements as a function of red cell concentration over the range between 0.05% and 4% ($\eta_o = 2$ mPa s). The shear stress was $\eta_o \langle\dot{\gamma}\rangle = 0.076$ N/m^2 before flow stop.

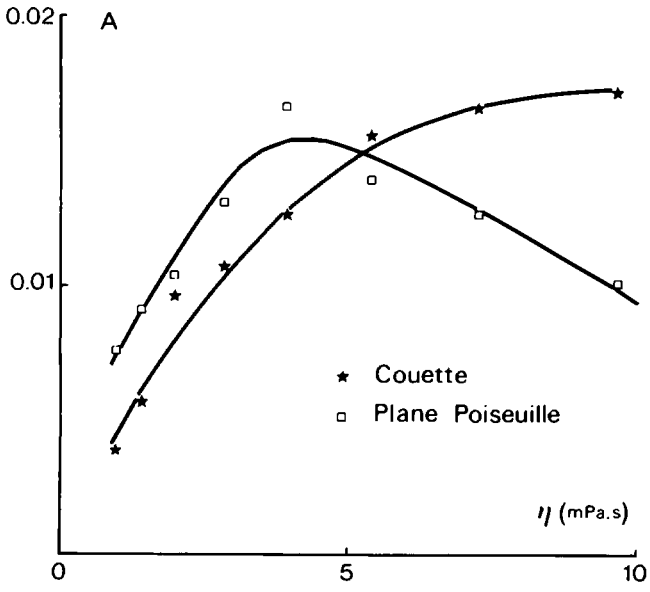

FIGURE 11 Slope of the straight lines (A) in Figs. 9 and 10 vs. suspending medium viscosity.

Orientation Rate

In the section Light Flux Measurements, we showed that one can assess the proportion of red cells in orbit $C = 0$ among the other possible orientations by measuring the ratio $\Delta r_{C-0}/\Delta r_T$ at an angle $\theta' \simeq 5°$. To evaluate the influence of rheological conditions on these proportions of erythrocytes in orbit $C = 0$, we plotted $\Delta r_{C-0}/\Delta r_T$ vs. $\eta_o \langle\dot{\gamma}\rangle$ for several suspending medium viscosities (Fig. 14). One can observe in this figure that whereas $\Delta r_{C-0}/\Delta r_T$ reaches a plateau at high shear stresses at very low values of η_o, it decreases monotonically with $\eta \langle\dot{\gamma}\rangle$ at increasing values of η_o. However, at $\eta_o \langle\dot{\gamma}\rangle \simeq 0.05$ N/m^2, $\Delta r_{C-0}/\Delta r_T \simeq 0.6$ irrespective of the viscosity η_o. It should be noted at this point that a critical phenomenon prevented us from extending our measurements toward higher values of the shear stress. Above a given threshold, a sudden transition of scattering pattern from the type of Fig. 5 *b* to that of Fig. 5 *c* occurred. Another author (H. L. Goldsmith, unpublished results) has considerable evidence that in Poiseuille flow, with $\eta_o = 20$ mPa s and $\dot{\gamma} > 4$ s^{-1}, cells in orbit $C > 0$ drift into a $C = 0$ orbit which gradually becomes a tank-treading motion. The red cells then align with the flow and are deformed into ellipsoids.

Finally, it is interesting to investigate the role of deformability in this process of RBC drift towards orbit $C = 0$. This was carried out by studying the effect of

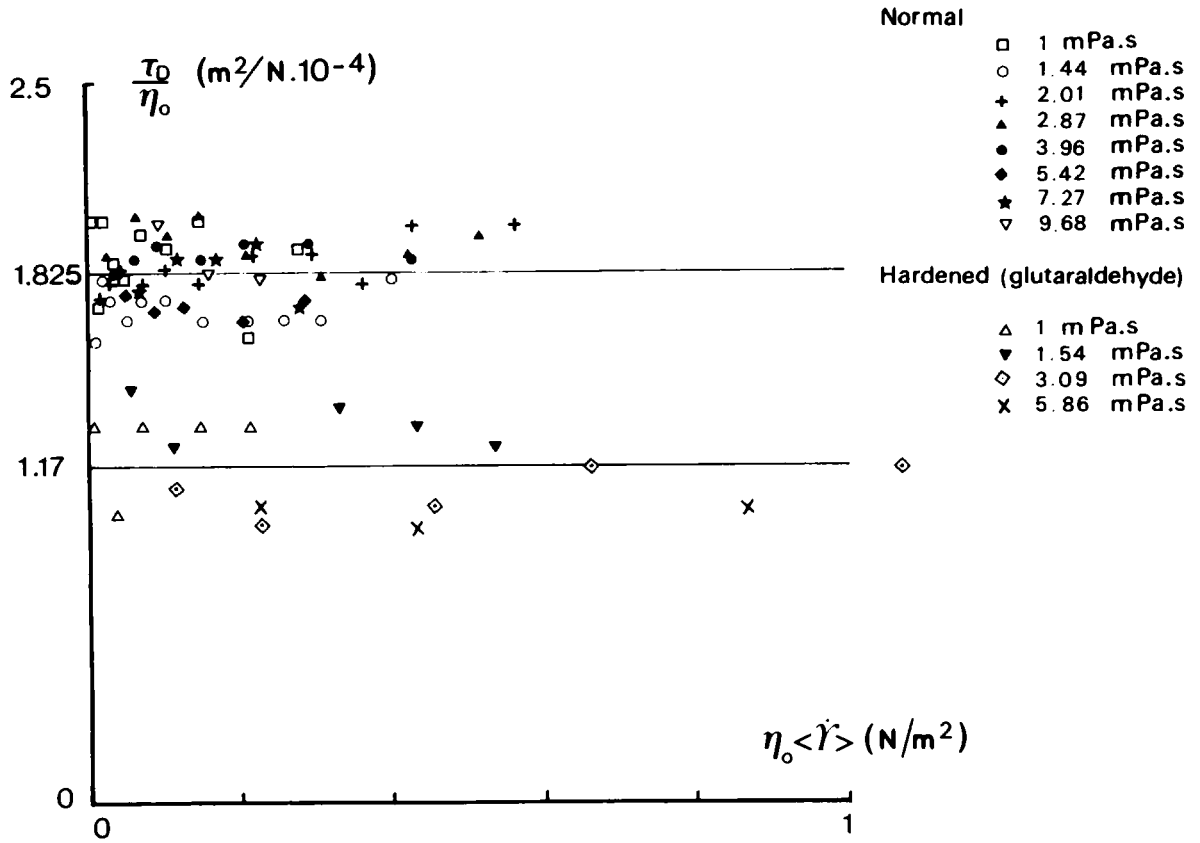

FIGURE 12 Disorientation time (related to η_0) vs. shear stress, for normal and hardened red cells.

alterations in membrane viscoelastic properties. Red cell heating and diamide treatment have qualitatively the same effect: they both decrease the proportion of erythrocytes which are able to settle in orbit $C = 0$. In Fig. 15, this proportion (assessed through $\Delta r_{C-0}/\Delta r_T$) is plotted vs. $\dot{\gamma}$, for several heating durations. The temperature of heating is 48.7 ± 0.2°C and the suspending medium viscosity $\eta_0 = 2$ mPa s. It can be seen that the longer the heating duration

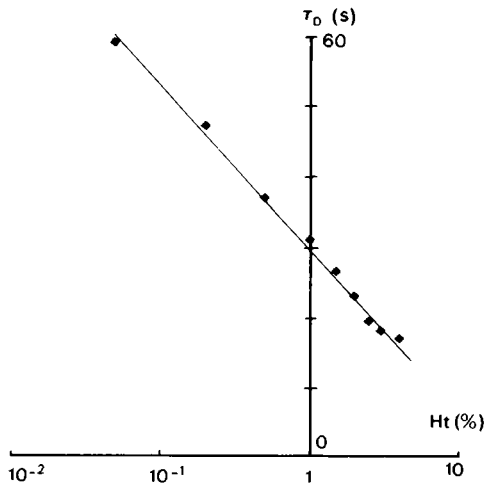

FIGURE 13 Disorientation time vs. hematocrit. $\eta_0 = 2$ mPa s; $\eta_0\langle\dot{\gamma}\rangle = 0.076$ N/m² before stop flow.

the lower $\Delta r_{C-0}/\Delta r_T$, especially at low shear rates. The data concerning the orientation of the RBCs after diamide treatment are plotted in Fig. 16. The suspending medium viscosity is $\eta_0 = 1$ mPa s, and the diamide concentration is varied between 0 and 0.2 mM. According to Fig. 16, the effect of spectra network cross-linking remains negligible on $\Delta r_{C-0}/\Delta r_T$ under 0.1 mM of diamide concentration. At 0.2 mM however, $\Delta r_{C-0}/\Delta r_T$ is lowered when compared to the intact erythrocytes irrespective of the shear rate.

DISCUSSION

The present results demonstrate some aspects of the relationship between RBC deformability and the behavior of cells in orbit $C = 0$. The drift of red cells in dilute suspensions from tumbling motion to stable spinning in orbit $C = 0$ and then from orbit $C = 0$ to parallel orientation with tank-treading are sensitive to alterations in membrane mechanical properties and could be used as a method for assessing such properties. However, the way deformable discoid objects such as erythrocytes drift towards orbit $C = 0$ in a time proportional to $\dot{\gamma}^{-1}$ and the mechanism by which they get back to random orientation after stop flow are not well understood. A complete hydrodynamic explanation of these processes would presumably be very involved, therefore in this discussion we will only suggest the main directions it should take.

(*A*) The simple proportionality we found between the

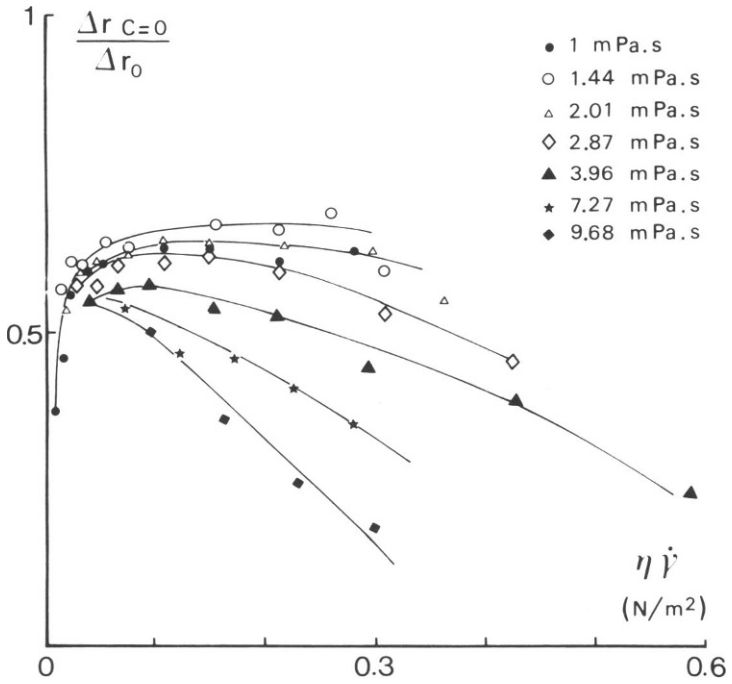

FIGURE 14 Red cell orientation rate in orbit $C = 0$ vs. shear stress, for several suspending medium viscosities.

orbital drift duration τ_0 and the inverse of shear rate $\dot{\gamma}^{-1}$ is a significant result. Indeed, no theory bearing on rigid particle motion in a flow is able to account for this dependence (see the section entitled "The Orbital Motion of a Rigid Ellipsoid or Disk"). Moreover, the order of magnitude of τ_0 ($\sim$10 s at $\langle\dot{\gamma}\rangle \simeq 10\,s^{-1}$ for $\eta_0 = 1$ mPa s) is much lower than the characteristic time of Eq. 4. Taking the typical half thickness and half diameter of an erythrocyte to be respectively $a \simeq 1\ \mu$m and $b \simeq 4\ \mu$m with $\dot{\gamma} = 10\ s^{-1}$, we obtain

$$-\frac{\eta_0}{\rho(a-b)a\dot{\gamma}^2} \simeq 3{,}000\ \text{s}.$$

This estimate is a lower bound, because $f(C/a)$ is generally <1 (14).

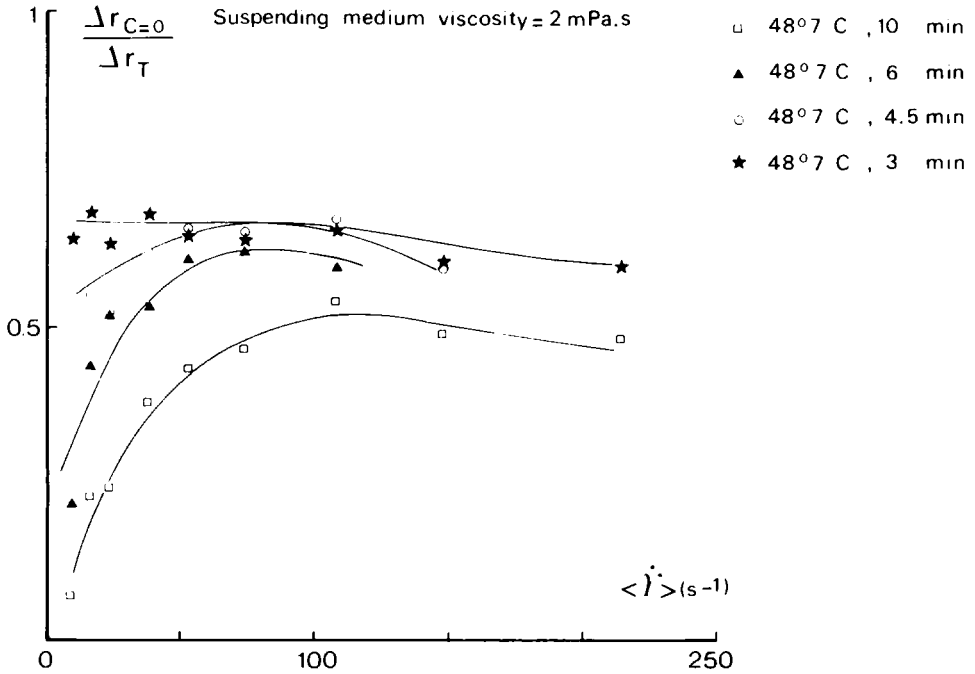

FIGURE 15 Orientation rate in orbit $C = 0$, vs. shear rate, for heat- treated cells.

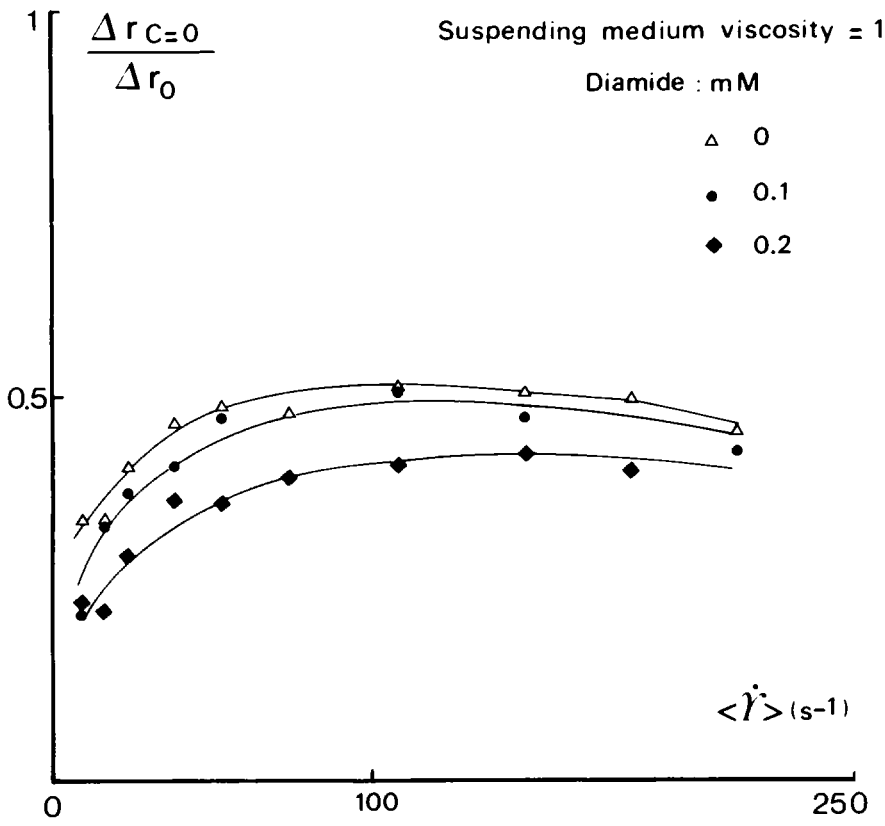

FIGURE 16 Orientation rate in orbit $C = 0$, vs. shear rate, for diamide- treated cells.

This problem is probably related to that of particle lateral migration in a flow that is bounded by walls. The latter assertion is made likely by the strong similarities in theoretical descriptions of these phenomena. It was first demonstrated by Bretherton (12) that the time reversal symmetry theorem for orbital drift in Stokes flow applies equally well to the lateral migration process. This led in turn to the introduction of first order inertial forces to account for the rigid particle lateral migration at low Reynolds number (23, 24). But when the topic of lateral migration of deformable particles was considered theoretically (25), it became clear that the first order inertial term is negligible at low Reynolds number when compared to the pure viscous forces. In fact, for deformable particles, the migration viscous force is proportional to the absolute magnitude of shear rate. In this case, the shear rate sign inversion does not require migration velocity reversal. We suggest that a similar argument should be applied to deformable particles in orbital drift. This would make it possible to develop a theoretical description in which the suspending fluid motion is described by the Stokes equation.

(*B*) We now consider the disorientation process and its connection with Brownian motion. The exact magnitude of the Brownian correlation time of an oblate ellipsoid having the same axis ratio r_e and the same diameter $2\ b$ as a human erythrocyte can be calculated exactly. In the case of a pure Brownian process, we can write (26)

$$\frac{\tau_B}{\eta_o} = \frac{16\Pi}{3k_BT}\,\frac{a^4 - b^4}{(2a^2 - b^2)S - 2a},$$

with

$$S = \frac{2}{(b^2 - a^2)^{1/2}} \cdot \tan^{-1}\frac{(b^2 - a^2)^{1/2}}{a}.$$

At $T = 300°K$, we find $\tau_B/\eta_o \simeq 9.8 \times 10^4\ m^2/N$. This is five times larger than the measured value: $\tau_D/\eta_o = 1.825 \times 10^4\ m^2/N$. Hence, it is clear that the facts do not support the Brownian description of red cell disorientation, even though the suspensions we used were quite dilute. Another explanation is needed. The observations of Jay and Canham (27, 28) on orientational stability of red cells during sedimentation in very dilute suspensions suggest one possible mechanism for the disorientation process. Sedimentation is, like Brownian motion, a process characterized by a constant ratio of time and viscosity. According to Jay and Canham, the erythrocytes suspended at hematocrit 0.01% in Ringer's solution at room temperature undergo random orientation changes during the sedimentation process. They set themselves alternately parallel, oblique, or perpendicular to the gravitational field. The average time between two such orientation changes is on the order of 20 s. This yields a ratio $\tau_D/\eta_o \simeq 2 \times 10^4\ m^2/N$, quite close to

our measured value. However, there is one disparity between the observations of Jay and Canham and the present results. For the sedimentation process, it was found that the average number of orientation changes per unit time was smaller when the RBCs were hardened than when they were deformable. In contrast, our results (Fig. 12) indicate that the disorientation rate (τ_D^{-1}) is higher (at given η_o) when the RBCs have been hardened than when they are deformable. This disparity could be due to the nonrandom initial orientation of the cells in our experiments. Immediately after flow stop, hardened cells are predominantly oblique with respect to the gravitational field, whereas deformable cells are either perpendicular (orbit $C = 0$) or parallel to it. Because the oblique position is far less lasting than the edge-on or face-on position (27), we would expect the disorientation time we measured to be shorter for hardened erythrocytes than for deformable ones.

The results shown in Fig. 13 that τ_D is a decreasing function of hematocrit suggest that long range hydrodynamic interactions between red cells are also important in the disorientation process. According to Batchelor's estimate (29), the fluid velocity perturbation yielded by the fall of a particle is $(\delta U/U_o) \sim (a'/R)$, where U_o is the sedimentation velocity, a' the particle radius, and R the average distance between two particles. The corresponding characteristic time is $\tau \sim (a'/\delta U) = (R/U_o) = (a'/U_o)$ $c^{-1/3}$ where c is the particle volume concentration. This result suggests that the sedimentation (disorientation) time should be a monotonically decreasing function of particle concentration, in qualitative agreement with the trends shown in Fig. 13. However, the dependence $\tau \sim c^{-1/3}$ was not observed. The latter discrepancy could be due to the differences in behavior which are to be expected when R is not equal to its average value, but is distributed over a range of possible values (29).

(*C*) The diameter increase we measured under the rheoscope when erythrocytes are in orbit $C = 0$ can be accounted for by a simple model of viscoelastic particles submitted to a shear stress, and having a circular cross-section at rest in the plane perpendicular to the vorticity vector (30). As shown in the latter paper, the maximum relative deformation that such a particle can undergo is approximately equal to the inverse of the viscosity ratio Λ: $\Lambda^{-1} = (\eta_o/\eta_m)$, where η_m is an effective particle viscosity. The shear rate $\dot{\gamma}_d$ at which 95% of such a deformation is reached is $\dot{\gamma}_d \simeq 3t^{-1}$, where t is the relaxation time of the deformation. For red blood cells, $t \simeq 0.1$ s (31) and $\eta_m \simeq 60$ mPa s to 100 mPa s. This effective viscosity is obtained by considering the ratio of dissipated energies

$$\frac{\dot{E}_M}{\dot{E}_C} = \frac{\eta_M \dot{\gamma}^2{}_M S}{\eta_C \dot{\gamma}^2{}_C V},$$

where η_M is the membrane surface viscosity, η_C the cytoplasmic viscosity, S the cell surface, and V the cell volume. Assuming that, during the red cell deformation relaxation process, $\dot{\gamma}_M$ is of the same order of magnitude as $\dot{\gamma}_C$, $\eta_M \simeq 0.5 \times 10^{-4}$ mPa s $\times$ m (32), at high shear stress for young cells and $\eta_C \simeq 6$ mPa s (33), we are led[2] to $\dot{E}_M/\dot{E}_C \simeq 10$.[2] This means that, to take into account the overall dissipative properties of the erythrocytes, we must choose an effective viscosity about ten times larger than cytoplasmic viscosity, i.e. $\eta_m \simeq 60$ mPa s (34). With such values and $\eta_o \simeq 7$ mPa s, the maximum RBC deformation in orbit $C = 0$ is on the order of 10% of the initial diameter. Moreover, the shear rate $\dot{\gamma}_d$ is $\simeq 20\ s^{-1}$ irrespective of η_o value. These theoretical predictions are in quite good agreement with the results presented in Fig. 4.

(*D*) The results shown in Fig. 11 indicate that the pattern of flow (Couette or Poiseuille) affects the process of orbital drift. The product $\tau_o^{-1}\dot{\gamma}^{-1}$ (or $\tau_o^{-1}\langle\dot{\gamma}\rangle^{-1}$) denoted by A, exhibits two distinct behaviors according to the flow pattern: it increases monotonically with η_o for Couette flow, whereas it begins to decrease above $\eta_o \simeq 5$ mPa s for Poiseuille flow. An explanation for this phenomenon may be found by considering the lateral migration of red blood cells away from the walls. If erythrocytes were to migrate towards the center of the gap in the Couette device, the shear rate they undergo would be essentially the same as near the walls. On the other hand, lateral migration of erythrocytes toward the center-line of a plane Poiseuille velocity profile would result in a decrease of the shear rate that the cells experience. The lateral migration velocity of flexible particles is a steep increasing function of the suspending medium viscosity (25, 35). When η_o has a low value, the red cells in Poiseuille flow are then likely to undergo orbital drift before they migrate appreciably toward the low shear rate region. In this case, the average shear rate $\langle\dot{\gamma}\rangle$ would be a good estimate of the actual shear rate experienced by the erythrocytes and the value of $\tau_o^{-1}\langle\dot{\gamma}\rangle^{-1}$ would parallel $\tau_o^{-1}\dot{\gamma}^{-1}$. However, if η_o is large, the lateral migration process could occur in the same time or even more rapidly than the orbital drift. In this case, the actual shear rate experienced by the red cells during orbital drift would be lower than $\langle\dot{\gamma}\rangle$, resulting in lower values for τ_o^{-1} and $\tau_o^{-1}\langle\dot{\gamma}\rangle^{-1}$.

I thank Dr. Feo from the Institut de Pathologie Cellulaire, Hopital de Bicêtre, 94270 - Kremlin Bicêtre (France) for providing me the opportu-

[2]These two assumptions need some words of comment:
(*a*) $\dot{\gamma}_M$ can only be considered of the order of magnitude as $\dot{\gamma}_c$ in the type of hydrodynamic situation assumed presently (i.e. R.B.C. spinning in orbit $C = 0$, or relaxation of an elongated R.B.C.: See reference 32). When, instead, the R.B.C. experiences a tank-treading motion, $\dot{\gamma}_M < \dot{\gamma}_c$. As evidenced by Fischer (36), one obtains a ratio $\dot{E}_M/\dot{E}_c = 1$ in this case.
(*b*) The value of η_M obtained by studying the time of extensional recovery of a whole R.B.C. (See reference 32.) was $\simeq 6 \times 10^{-4}$ mPa s $\times$ m, leading to $\dot{E}_M/\dot{E}_c = 10^2$. But this estimate, as well as that given by the micropipette recovery-time technique, is probably an upper bound, due to the averaging over relaxation curves including at least two time constants (See reference 37 and the Discussion in reference 33.). If the first time constant is taken into account, the value 0.6×10^{-4} mPa s $\times$ m is found (37), in quite good agreement with (33).

nity to use a rheoscope and an ektacytometer, and for accurately discussing the meaning of the measurements performed with these devices. I acknowledge the referees and the editor for their very useful comments and their efforts to achieve greater clarity in the expression of this difficult topic. Moreover, I wish to thank Dr. H. Goldsmith for his thorough suggestions, and for having allowed me to include reference to many unpublished results from his extensive work on RBC orientation. Finally, I thank Miss Mériou for her efficient secretarial asssistance.

Received for publication 26 December 1984 and in final form 25 November 1985.

REFERENCES

1. Goldsmith, H. L. 1971. Deformation of human red cells in tube flow. *Biorheology.* 7:235–242.
2. Fischer, T., and H. Schmid-Schonbein. 1977. Tank treading motion of red cell membrane in viscometric flow: behavior of intra cellular and extra cellular markers (with film). *Blood Cells.* 3:351–365.
3. Fischer, T., M. Stohr, and H. Schmid-Schonbein. 1978. RBC microrheology: comparison of the behaviour of single RBC and liquid droplet in shear flow. *Ai. Ch. E. Symp. Ser. n° 182.* 74:38–45.
4. Kholeif, I. A., and H. D. Weymann. 1974. Motion of a single RBC in plane shear flow. *Biorheology.* 11:337–348.
5. Keller, S. R., and R. Skalak. 1982. Motion of a tank-treading ellipsoidal particle in a shear flow. *J. Fluid Mech.* 120:27–47.
6. Secomb, T. W., T. Fisher, and R. Skalak. 1983. The motion of close packed red cells in shear flow. *Biorheology.* 20:295–309.
7. Bitbol, M., and F. Leterrier. 1982. Measurement of erythrocyte orientation in flow by spin labeling. I. Comparison between experimental and numerically simulated EPR spectra. *Biorheology.* 19:669–680.
8. Bitbol, M., F. Leterrier, J. Dufaux, and D. Quemada. 1985. Measurement of erythrocyte orientation in flow by spin labeling. III. Erythrocyte orientation and rheological conditions. *Biorheology.* 22:43–53.
9. Goldsmith, H. L., and J. Marlow. 1972. Flow behaviour of erythrocytes. I. Rotation and deformation in dilute suspensions. *Proc. R. Soc. Lond. B. Biol. Sci.* 182:351–384.
10. Jeffery, G. B. 1922. The motion of ellipsoidal particles immersed in a viscous fluid. *Proc. R. Soc. Lond. A. Biol. Sci.* 102:161–179.
11. Trevelyan, B. J., and S. G. Mason. 1951. Particle motion in sheared suspensions. I. Rotations. *J. Coll. Sci.* 6:355–367.
12. Bretherton, F. P. 1962. The motion of rigid particles in a shear flow at low Reynolds number. *J. Fluid Mech.* 14:284–304.
13. Goldsmith, H. L., and S. G. Mason. 1967. The microrheology of dispersions. *In* Rheology, Theory, and Applications. Vol. IV. F. R. Eirich, editor. Academic Press, Inc., New York. 85–250.
14. Saffman, P. G. 1956. On the motion of small spheroidal particles in a viscous liquid. *J. Fluid. Mech.* 1:540–553.
15. Karnis, A., H. L. Goldsmith, and S. G. Mason. 1966. The flow suspensions through tubes. V. Inertial effects. *Can. J. Chem. Eng.* 44:181–193.
16. Morel, F. M. M., R. F. Baker, and H. Wayland. 1971. Quantitation of human red blood cell fixation by glutaraldehyde. *J. Cell. Biol.* 48:91–100.
17. Fischer, T. M., C. W. M. Haest, M. Stohr, D. Kamp, and B. Deuticke. 1978. Selective alteration of erythrocyte deformability by SH reagents. *Biochim. Biophys. Acta.* 510:270–282.
18. Rakow, A. L., and R. M. Hochmuth. 1975. Effect of heat treatment on the elasticity of human erythrocyte membrane. *Biophys. J.* 15:1095–1100.
19. Korpman, R. A., D. C. Dorrough, and J. D. Brailsford, and B. S. Bull. 1977. The red cell shape as an indication of membrane structure, Ponder's rule reexamined. *Blood Cells.* 3:315–344.
20. Bessis, M., and N. Mohandas. 1975. A diffractometric method for the measurement of cellular deformability. *Blood Cells.* 1:307–313.
21. Ravey, J. C. 1983. Diffusion de la lumière: application aux particules de grande taille comme les globules rouges. Techniques avancées en hémorhéologie. M. L. Viriot, J. C. André, M. Lucius, and J. F. Stoltz, editors. DPIC-INPL, Nancy. 505–542.
22. Okagawa, A., and S. G. Mason. 1977. Kinetics of flowing dispersions X. *Can. J. Chem.* 55:4243–4256.
23. Cox, R. G., and H. Brenner. 1968. The lateral migration of solid particles in Poiseuille flow. I. Theory. *Chem. Eng. Sci.* 23:147–173.
24. Cox, R. G., and S. K. Hsu. 19xx. The lateral migration of solid particles in a lamination flow in a plane. *Int. J. Multiphase Flow.* 3:201–217.
25. Chan, P. C. H., and L. G. Leal. 1979. The motion of a deformable drop in a second order fluid. *J. Fluid Mech.* 131–170.
26. Perrin, F. 1934. Mouvement Brownien d'un ellipsoîde. I. Dispersion diélectrique pour des molécules éllipsoîdale. *J. Phys. et Radium.* 5:Série 7:497–511.
27. Jay, A. W. L., and P. B. Canham. 1973. Sedimentation of single human red blood cells. Differences between normal and glutaraldehyde fixed cells. *J. Cell. Physiol.* 80:367–372.
28. Canham, P. B., A. W. L. Jay, and E. Tilsworth. 1971. The rate of sedimentation of individual human red blood cells. *J. Cell. Physiol.* 78:319–322.
29. Batchelor, G. K. 1972. Sedimentation in a dilute dispersion of spheres. *J. Fluid Mech.* 52:245–268.
30. Bitbol, M., and P. Mills. 1984. The deformation of a viscoelastic sphere in a time dependent shear flow. *J. Physique Lett.* 45:L775–780.
31. Evans, E. A., and R. Skalak. 1980. Mechanics and thermodynamics of biomembranes. CRC Press, Inc. Boca Raton, FL
32. Transontay, R., S. P. Sutera, and P. R. Rao. 1984. Determination of RBC membrane viscosity from rheoscopic observations of tank-treading motion. *Biophys. J.* 46:65–72.
33. Chien, S. 1977. Rheology of sickle cells and erythrocyte content. *Blood Cells.* 3:283–303.
34. Goldmsith, H. L. 1971. Red cells motions and wall interations in tube flow. *Fed. Proc.* 30:1578–1588.
35. Fischer, T. M. 1980. On the energy dissipation in a tank treading human red blood cell. *Biophys. J.* 32:863–868.
36. Chien, S., K. L. P. Sung, R. Skalak, S. Usami, and A. Tozeren. 1978. Theoretical and experimental studies on viscoelastic properties of erythrocyte membrane. *Biophys. J.* 24:463–487.